第34卷 第5期 焊 接 学 报 Vol. 34 No. 5
2013年5月 TRANSACTIONS OF THE CHINA WELDING INSTITUTION May 2013

热输入对Q500CF钢板焊接热影响区组织和冲击性能的影响

郭慧英， 张 宇， 何玉春， 许红梅
(江苏省(沙钢)钢铁研究院，张家港 215625)

摘 要：通过埋弧焊试验和Gleeble热模拟试验研究了热输入对Q500CF钢热影响区(HAZ)组织和冲击性能的影响. 埋弧焊结果表明，热输入为15～50 kJ/cm时，HAZ的-20 ℃冲击吸收功大于等于146 J；HAZ中熔合线(FL)处冲击吸收功最低且随热输入增大而减小. 组织观察表明，随热输入增加，粗晶区组织由15 kJ/cm时的板条贝氏体(LB)和粒状贝氏体(GB)转变为50 kJ/cm时的GB组织；临界粗晶区在晶界上出现了大量1～7 μm的M-A组元，导致低温冲击韧性恶化. Gleeble热模拟结果表明，热输入为50～70 kJ/cm时，粗晶区GB组织粗化并导致该区冲击韧性恶化. 因此为确保多道焊焊接接头HAZ低温冲击韧性，焊接热输入应限制在15～50 kJ/cm之间.

关键词：低焊接裂纹敏感性钢；埋弧焊；粗晶热影响区；热模拟；冲击性能
中图分类号：TG457.11 **文献标识码**：A **文章编号**：0253-360X(2013)05-0108-05

郭慧英

0 序 言

为了简化焊接工艺，提高效率，低焊接裂纹敏感性高强钢(简称CF钢)被广泛应用于水电站压力钢管、工程机械、压力容器等对焊接性要求较高的领域[1-3]. 该钢种在不预热或低预热的情况下不出现焊接裂纹，具有低裂纹敏感性、高强高韧性. 为满足国内基建用钢的需求，沙钢利用先进的控轧控冷工艺，自主研制了抗拉强度610 MPa级CF钢(Q500CF)，厚度大于等于60 mm的钢板可实现热轧态交货，钢板综合性能优良，兼顾了高强度和优良的低温冲击韧性. 为考察该钢种的焊接性能，并涵盖其施工中常用的焊条电弧焊、气体保护焊和埋弧焊的热输入范围[4,5]，特进行了埋弧焊试验并借助Gleeble热模拟试验，着重分析了热输入对焊接热影响区组织和冲击性能的影响，从而给工程建设中焊接工艺的制定提供参考.

1 试验方法

试验材料为40 mm厚热轧态Q500CF钢板，其成分为(质量分数，%) C 0.06，Si 0.26，Mn 1.46，P 0.006 5，S 0.003 5，Ti 0.015，Nb 0.04，以及适量的Ni，Cr，Mo和V等，焊接裂纹敏感性指数P_{cm}≤0.20%；钢板组织见图1，屈服强度≥515 MPa，抗拉强度≥625 MPa，-20 ℃冲击吸收功>200 J. 埋弧焊所用焊材为H08C焊丝(ϕ 4.0 mm)和SJ101焊剂.

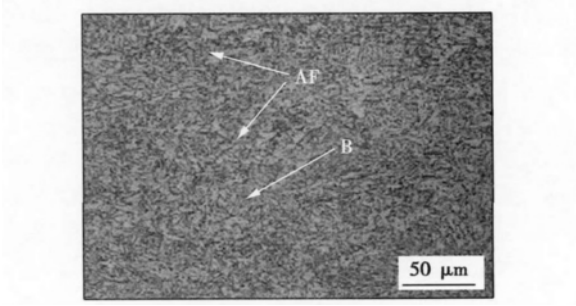

图1 母材钢板光学显微组织
Fig. 1 Optical microstructure of base metal Q500CF

焊接试板采用对称双面V形60°坡口，钝边为5 mm；焊前不预热，无焊后热处理，层间温度≤150 ℃. 焊接工艺参数见表1.

焊接热模拟在Gleeble 3800上进行，一次热循环粗晶热影响区(CGHAZ)模拟参数如下. (1)以150 ℃/s的速度加热到峰值温度1 350 ℃并停留2 s；(2)采用3D热源传热模型；(3)焊接热输入设定为15，25，35，50和70 kJ/cm. 为研究多道焊过程中热影响区的组织及性能变化规律，进行二次热循环

收稿日期：2012-04-28

表 1　埋弧焊工艺参数

Table 1　Welding parameters of SAW

热输入 E/(kJ·cm^{-1})	焊接电流 I/A	电弧电压 U/V	焊接速度 v/(cm·min^{-1})
15	450	29	52.2
50	750	36	32.4

的热模拟试验，主要模拟临界粗晶热影响区（IC-CGHAZ），二次热循环的峰值温度为 780 ℃并停留 0.5 s，其它设置同前.

用 Zeiss 光学显微镜观察金相组织，JEOL JSM 7001F 场发射扫描电子显微镜观察精细组织及冲击试样断口形貌. 低温冲击试验在 Instron 冲击试验机上进行，采用 10 mm×10 mm×55 mm 标准尺寸. 维氏硬度在 Instron 维氏硬度计上完成，载荷为 49 N.

2　试验结果分析与讨论

2.1　埋弧焊接头低倍形貌

接头横截面低倍形貌见图 2，组织观察未发现气孔裂纹等缺陷，接头质量完好.

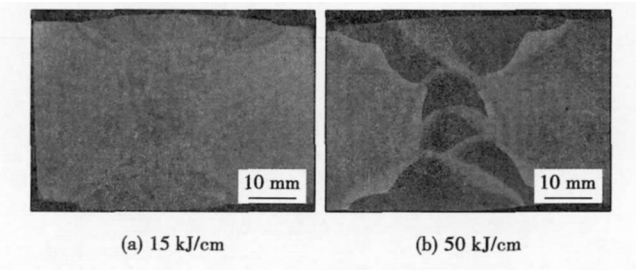

图 2　焊接接头横截面低倍形貌

Fig. 2　Cross-sections of welded joints

2.2　埋弧焊接头热影响区组织

图 3 为焊接热输入 15 和 50 kJ/cm 下埋弧焊接头的 CGHAZ 和 ICCGHAZ 区域的微观组织. 图 3a 和 3b 对比可知，15 kJ/cm 焊接接头的 CGHAZ 由板条贝氏体(LB)和粒状贝氏体(GB)构成，当热输入增加到 50 kJ/cm 时，CGHAZ 主要由 GB 构成，并且 GB 明显粗化. 与 CGHAZ 相比较，ICCGHAZ 组织中出现了沿原奥氏体晶界分布的 M-A 组元（箭头所示），其典型形貌见图 4，尺寸在 1 ~ 7 μm.

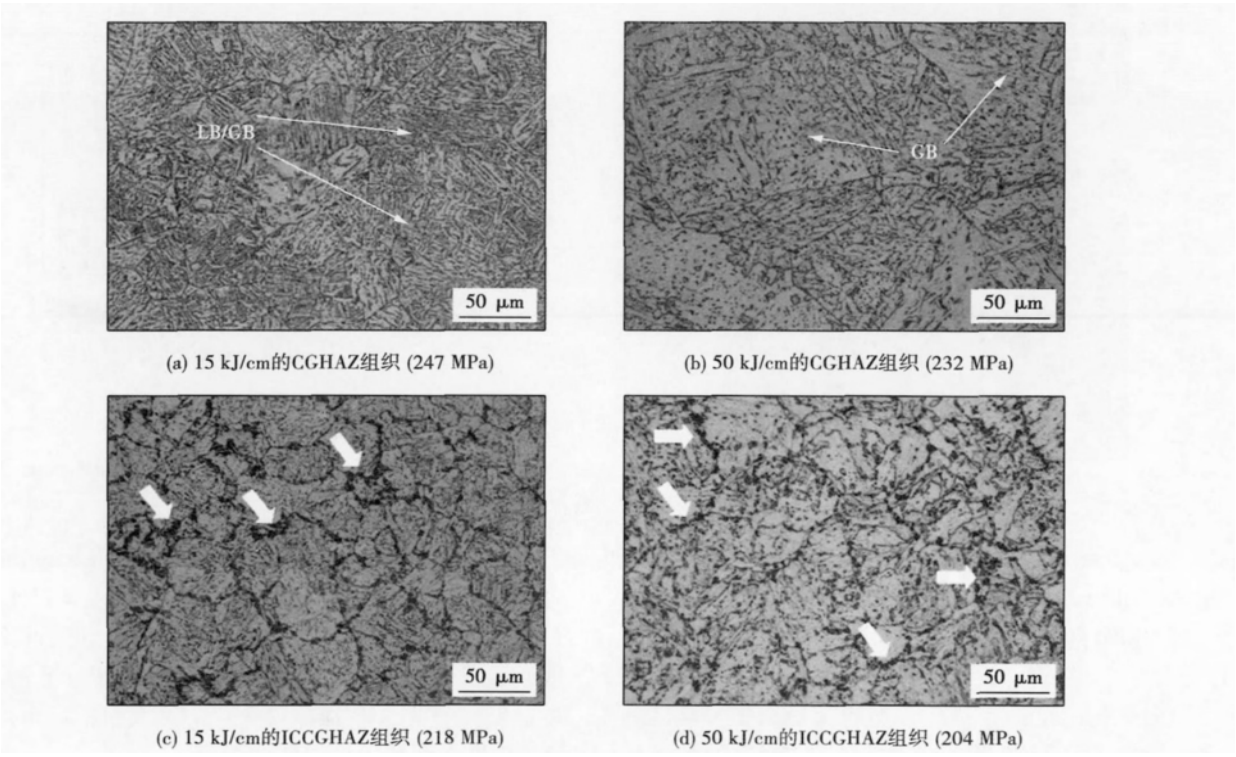

图 3　焊接接头 HAZ 组织

Fig. 3　Optical microstructure of HAZ in welded joints

细晶热影响区(FGHAZ)主要由尺寸细小的多边形铁素体(PF)构成，该区域硬度值为 191 MPa，与母材接近；而临界热影响区(ICHAZ)则由 PF、未转变的母材组织以及部分第二相组成，各相体积含量

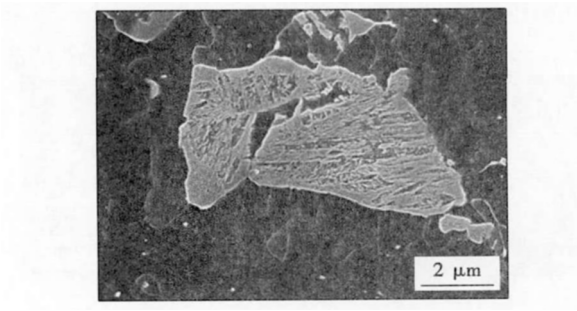

图 4 ICCGHAZ 中的典型 M-A 组元形貌

Fig. 4 Typical morphology of M-A constituents

随位置变化而变化，该区域硬度值为 188 MPa，比母材略低；热输入为 15 和 50 kJ/cm 的焊接接头中，FGHAZ 和 ICHAZ 组织特征类似（图 5），但组织梯度和区域宽度随热输入增大而增大.

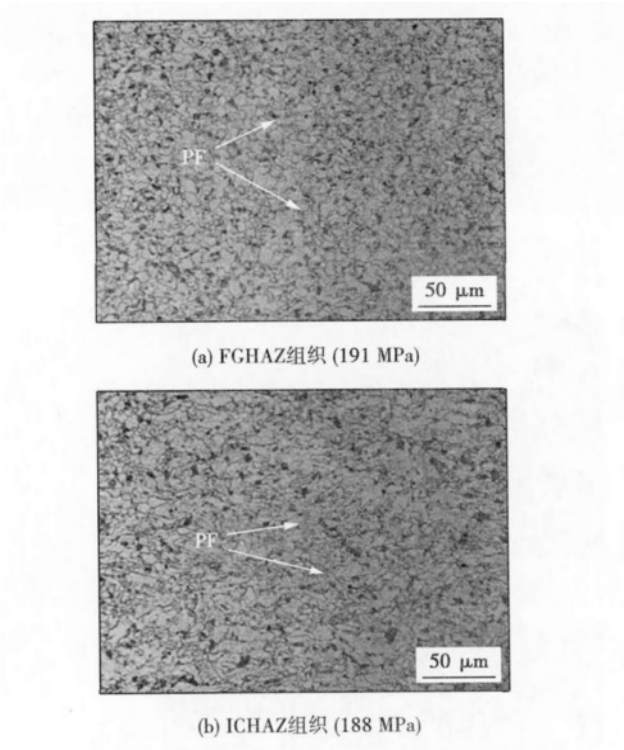

图 5 50 kJ/cm 的接头 FGHAZ 与 ICHAZ 组织

Fig. 5 Microstructure of FGHAZ and ICHAZ of 50 kJ/cm weld joint

表 2 列出了焊接热输入对焊接接头热影响区各区域宽度的统计结果. 由表 2 可见，HAZ 的各区域宽度随热输入增加均相对增加，CGHAZ 宽度由 15 kJ/cm 时的 1.5 mm 增加到 50 kJ/cm 时的 2.6 mm. 由于 ICCGHAZ 区域由前一道次的 CGHAZ 和后一道次的 ICHAZ 叠加而成，因此 ICCGHAZ 在整个 HAZ 区域中的体积含量也将随热输入增加而增加；由于该区域为局部脆性区，这势必造成多道次焊接接头 HAZ 冲击性能随热输入的增加而下降.

表 2 热影响区各区域平均宽度（d/mm）

Table 2 Width of regions across HAZ

热输入 E/(kJ·cm^{-1})	CGHAZ	FGHAZ	ICHAZ
15	1.5	0.8	0.6
50	2.6	1.0	1.1

2.3 埋弧焊接头热影响区冲击性能

图 6 示出了热输入为 15 和 50 kJ/cm 的埋弧焊接头热影响区的冲击性能，可看出：（1）熔合线（FL）和 FL+2 mm 位置处冲击吸收功随热输入增加而降低；（2）相同热输入下，FL 位置处冲击吸收功最低. FL+2 mm 位置对于 15 kJ/cm 的接头来说，处于 FGHAZ 区，而对于 50 kJ/cm 的接头来说则仍处于 CGHAZ 区，因此 50 kJ/cm 接头该区域的冲击性能较低[6-8]. FL+5 mm 处于 HAZ 之外，因此该区域的冲击性能不受热输入影响，其 −40 ℃ 的冲击吸收功 $A_{KV}\geqslant 214$ J，与母材（FL+20 mm 处）的冲击吸收功（$A_{KV,-40\,℃}\geqslant 25$ J）处于同一水平.

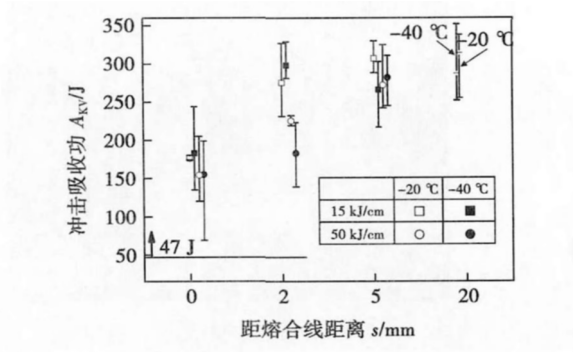

图 6 焊接接头 HAZ 冲击性能

Fig. 6 Impact property of HAZ of welded joints

由图 6 可知，在热输入为 15 和 50 kJ/cm 的条件下可得到满足 −40 ℃ 冲击韧性要求（$\geqslant$47 J）的焊接接头. 结合图 3 与图 6 可知，FL 位置处冲击吸收功最低是由 CGHAZ 区粗大的 GB 组织导致的；而随热输入增加，GB 组织尺寸相应增大（图 3a，b），导致 FL 位置处冲击性能相应降低.

2.4 焊接热模拟的组织与性能

为进一步探讨热输入量的变化对热影响区的组织和性能的影响规律，用 Gleeble 3800 模拟了焊接热影响区中性能最差的两个区域[9-11]（CGHAZ 和 ICCGHAZ）在不同热输入下的组织及性能.

图 7 和表 3 列出了热输入量对 CGHAZ 区域的组织和冲击性能的影响结果. 由图 7 可见: (1) 热输入为 15 ~ 35 kJ/cm 时,CGHAZ 主要由 LB 和 GB 构成; (2) 热输入为 50 ~ 70 kJ/cm 时,CGHAZ 由 GB 构成,且其尺寸随热输入增大而增大. 对比发现,图 7a 和图 7d 中模拟 CGHAZ 的形貌特征、组织类型与图 3a,3b 埋弧焊接头组织相似; 模拟 15 和 50 kJ/cm 热输入下的 CGHAZ 区域的硬度值为 253 MPa 和 220 MPa,与实际埋弧焊接头的硬度值 247 MPa 和 232 MPa 分别相差 6 MPa 和 12 MPa,比较接近,揭示了热模拟结果的可靠性.

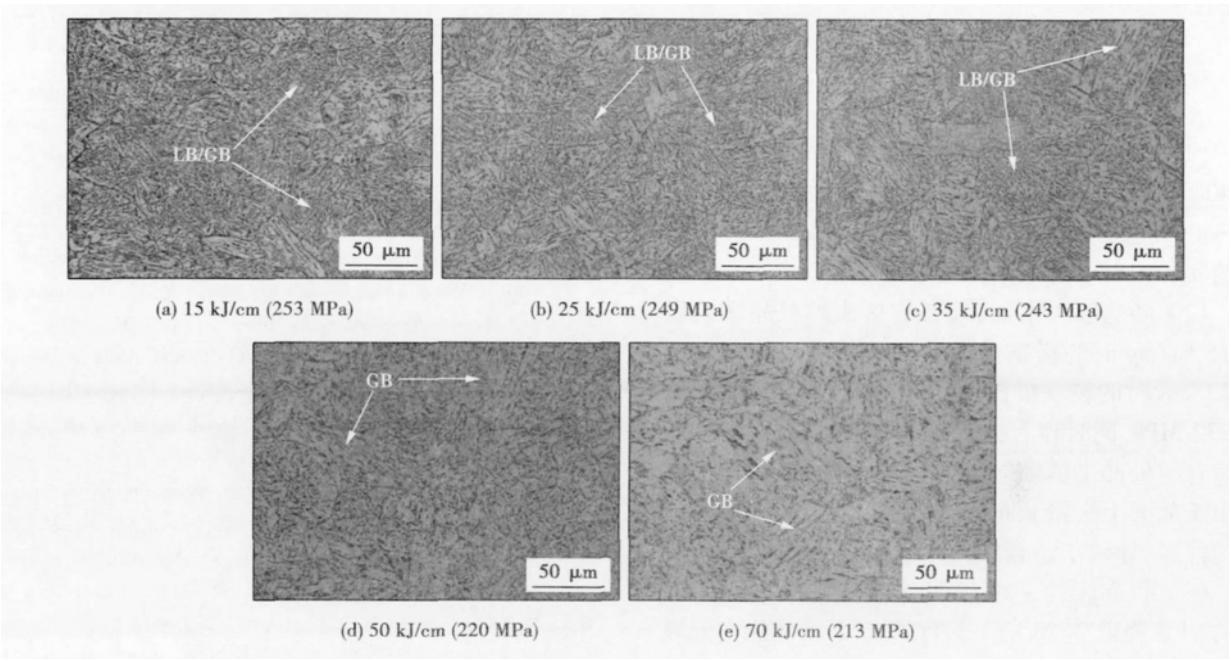

图 7　热模拟 CGHAZ 组织

Fig. 7　Optical microstructure of simulated CGHAZ

表 3　热模拟 CGHAZ 冲击吸收功

Table 3　Impact property of simulated CGHAZs

热输入 E/(kJ·cm^{-1})	冲击吸收功 $A_{KV,-20\,℃}$/J
15	221
25	168
35	103
50	91
70	17

由表 3 看出: (1) 热输入为 15 ~ 35 kJ/cm 时,CGHAZ 区 −20 ℃ 冲击吸收功 $A_{KV} \geqslant 103$ J; (2) 热输入为 50 kJ/cm 时,CGHAZ 的 −20 ℃ 冲击吸收功为 91 J; (3) 热输入为 70 kJ/cm 时,CGHAZ 的 −20 ℃ 冲击吸收功为 17 J. 热输入为 35 kJ/cm 的冲击试样的断口呈现准解理特征(图 8a),断裂单元(图 8a 中点划线)内部呈现脆性断裂特征,但断裂单元之间高低不一、撕裂痕迹明显,表明断裂过程中吸收了较多的能量; 而热输入为 70 kJ/cm 的冲击试样的断口解理特征明显,断裂单元(图 8b 点划线)在 50 ~ 60 mm 之间,断裂单元之间撕裂痕迹不明显.

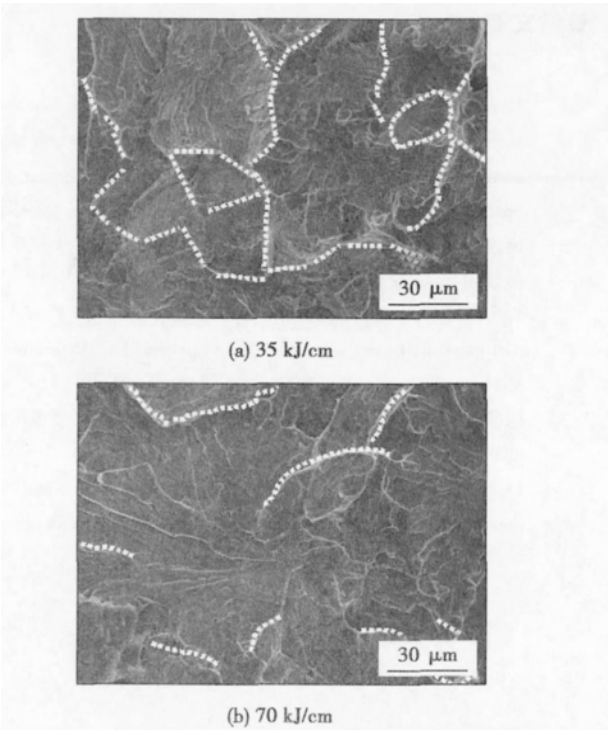

图 8　热模拟 CGHAZ 冲击断口形貌

Fig. 8　Morphology of fractured simulated CGHAZs after charpy impact test

热模拟的 ICCGHAZ 区 -20 ℃ 冲击吸收功 A_{KV} ≤21 J，在 15 ~ 70 kJ/cm 之间随热输入增大而减小，均不能满足对母材的要求(A_{KV} ≥47 J) . 此结果揭示粗晶区经 780 ℃ 二次热循环后性能恶化，为焊接接头热影响区的局部脆性区，降低了 FL 位置处的冲击吸收功.

3 结 论

(1) 无预热和焊后热处理可得到满足性能要求的 40 mm 厚 Q500CF 钢焊接接头，热输入为 15 ~ 50 kJ/cm 的埋弧焊接头的热影响区的 -20 ℃ 冲击吸收功 A_{KV} ≥146 J，满足对母材的要求.

(2) 随热输入增加，埋弧焊接头的粗晶区组织由 15 kJ/cm 时的板条贝氏体和粒状贝氏体转变为 50 kJ/cm 时的粒状贝氏体，硬度值由 247 MPa 降低到 232 MPa，同时伴有粒状贝氏体的粗化，这也导致了熔合线处冲击值随热输入增加而降低; 临界粗晶区由于晶界上大量分布的 M-A 组元，使该区成为局部脆性区，导致了熔合线处冲击吸收功的波动.

(3) 粗晶区的 -20 ℃ 冲击吸收功由 50 kJ/cm 时的 91 J 降低到 70 kJ/cm 时的 17 J，为确保实际焊接接头热影响区的低温冲击韧性，焊接热输入 E ≤ 50 kJ/cm.

参考文献:

[1] Hayashi Kenji, Araki Kiyomi, Abe Takashi. High performance steel plates for tank and pressure vessel use high strength steel plates with excellent weldability and superior toughness for the energy industry [J]. JFE Technical Report, 2005(5): 66-73.

[2] 姚连登. CF 钢在煤矿机械和水电工程中的应用现状及开发前景 [J]. 机械工程材料, 2004, 28(12): 39-41.
Yao Liandeng. Application and development trend of CF steel in coal mine machinery and hydroelectric project [J]. Materials for Mechanical Engineering, 2004, 28(12): 39-41.

[3] 陈颜堂，芮晓龙. 600 MPa 级高能量输入焊接压力钢管用钢的研制 [J]. 钢铁, 2007, 42(6): 38-41.
Chen Yantang, Rui Xiaolong. Development of 600 MPa steel for pressure tube welded with high heat input [J]. Iron & Steel, 2007, 42(6): 38-41.

[4] 陈 晓，秦晓钟. 高性能压力容器和压力钢管用钢 [M]. 北京: 机械工业出版社, 2007.

[5] 张一任，何前进，房务农，等. B610CF-L2 与 JFE-HITEN610U2L 钢焊接性能对比研究 [J]. 电焊机, 2012, 42(2): 74-78.
Zhang Yiren, He Qianjin, Fang Wunong, *et al*. Research and comparison about weldability of B610CF-L2 and JFE-HIT-EN610U2L steel [J]. Electric Welding Machine, 2012, 42(2): 74-78.

[6] Jang J, Lee J S, Ju J B, *et al*. Determination of microstructural criterion for cryogenic toughness variation in actual HAZs using microstructure-distribution maps [J]. Materials Science and Engineering A, 2003, 351(1/2): 183-189.

[7] Lambert P A, Gourhues A F, Besson J, *et al*. Mechanisms and modeling of cleavage fracture in simulated heat-affected zone microstructures of a high strength low alloy steel [J]. Metallurgical and Materials Transactions A, 2004, 35(3): 1039-1053.

[8] Shome M, Gupta O P, Mohanty O N. Effect of simulated thermal cycles on the microstructure of the heat-affected zone in HSLA-80 and HSLA-100 steel plates [J]. Metallurgical and Materials Transactions A, 2004, 35(3): 985-996.

[9] Bonnevie E, Ferriere G, Ikhlef, *et al*. Morphological aspects of martensite-austenite constituents in intercritical and coarse grain heat affected zones of structural steel [J]. Materials Science and Engineering A, 2004, 385(1/2): 352-358.

[10] 张英乔，张汉谦，刘伟民. M-A 组元对石油储罐用钢粗晶热影响区韧性的影响 [J]. 焊接学报, 2009, 30(1): 109-112.
Zhang Yingqiao, Zhang Hanqian, Liu Weimin. Effect of M-A constituent on toughness of coarse grain heat-affected zone in HSLA steels for oil tanks [J]. Transactions of the China Welding Institution, 2009, 30(1): 109-112.

[11] 荆洪阳，霍立兴，张玉凤. 铌对高强钢焊接热影响区中马氏体-奥氏体组元形态的影响 [J]. 焊接学报, 1997, 18(1): 37-42.
Jing Hongyang, Hou Lixing, Zhang Yufeng. Effect of niobium on morphology of martensite-austenite constituents in weld HAZ [J]. Transactions of the China Welding Institution, 1997, 18(1): 37-42.

作者简介: 郭慧英，女，1983 年出生，硕士. 主要从事钢板新品开发及配套焊接技术、材料的开发. 发表论文 5 篇. Email: guohy-iris@shasteel.cn

通讯作者: 张 宇，男，高级研究员. Email: zhangyu-iris@shasteel.cn

Abstract: Firstly, the thermo-electric coupling ANSYS model of multi-points projection welding is built up and the results reveal that the current has an apparent diversion phenomenon at different projection points. Due to the combined effects of temperature and pressure, the values of current density in the middle of contact points between the upper and lower workpieces are maximal and decrease distinctly on both sides. Then the thermal and electrical behavior of the metal corrugated plate packing with 0.17 mm thickness 304 stainless steel is quantitatively analyzed in the process of projection welding. Meanwhile, the temperature field in the nugget formation process has been obtained. The sizes of nugget obtained by numerical simulation are in good agreement with the measured results. Therefore, this method provides a theoretical basis for the design and optimization of the parameters in multi-point projection welding process.

Key words: multi-points projection welding; nugget; numerical simulation; metal corrugated plate packing

Full factorial design on triple-electrode high speed CO_2 fillet welding on double sides MA Xiaoli, LIN Hang, HUA Xueming, WU Yixiong (School of Material Science and Engineering, Shanghai JiaoTong University, Shanghai 200240, China). pp 95-98

Abstract: Multi-parameters have impact on the weld geometry during triple-electrode high speed CO_2 welding. All the parameters cannot be considered at one time. Therefore, the main parameters should be studied during the welding process. In this paper, two kinds of factors such as welding power and welding speed of three levels were studied to predict the weld geometry parameters by statistical method. The results show that the horizontal leg length, vertical leg length and the convexity degree are affected by the main effect. The predicted value of vertical leg length is 4 mm, the horizontal leg length is 2.5 mm, and the convexity degree is 2.5 mm.

Key words: triple-electrode CO_2 welding on double sides; welding power; welding speed; weld geometry parameters

Welding process stability evaluation of underwater wet manual metal arc welding HU Jiakun[1], WU Chuansong[1], JIA Chuanbao[2] (1. Key Lab for Solid-Liquid Structure Evolution and Materials Processing of the Education Ministry of China, Shandong University, Jinan 250061, China; 2. Shandong Provincial Key Laboratory of Special Welding Technology, Shandong Academy of Sciences Institute of Oceanographic Instrumentation, Qingdao 266001, China). pp 99-102

Abstract: Welding electrical parameters (arc voltage and welding current) include abundant information of welding procedure. This paper collects instantaneous value of arc voltage for underwater wet manual arc welding at different welding conditions, taking different depth and welding electrode for instance. And then, the instantaneous value of voltage was processed statistically. The process stability of underwater wet manual arc welding was analyzed visually and evaluated quantitatively based on standard deviation (σ_U), the combination of frequency distribution of the D-value (H) between instantaneous value and mean value of arc voltage with stability exponential (W). The result shows that the stability of different welding process could be well identified, which is very theoretically meaningful as giving a new method for stability control for underwater welding process.

Key words: underwater wet manual metal arc welding; statistical processing; welding process stability

Effect of P element on microstructure and properties of Al-Si-Zn filler metal ZHANG Shuai[1], XUE Songbai[1], YANG Jinlong[1], LOU Jiang[2], WANG Shuiqing[2] (1. College of Materials Science and Technology, Nanjing University of Aeronautics and Astronautics, Nanjing 210016, China; 2. Zhejiang Xinrui Welding Material Co., Ltd, Shengzhou 312452, China). pp 103-107

Abstract: The effect of P on the spreadability, microstructure of Al-Si-Zn filler metal and the mechanical properties of brazed joints were studied. Results show that the spreadability of the Al-Si-Zn filler metal was improved by the addition of P, and furthermore, both the plate shape primary silicon and needle shape eutectic silicon of the filler metal were refined effectively. Tensile tests indicate that the fracture position of lap joints locates at the base metal and butt joints locates at brazing seam respectively, and the tensile strength of the butt joint brazed with Al-Si-Zn filler metal increased firstly, and then decreased with the increasing of P addition. When the content of P was about 0.06%, the comprehensive properties of the Al-Si-Zn filler metal were the best.

Key words: P element; Al-Si-Zn filler metal; spreadability; microstructure; mechanical properties

Effect of heat input on microstructure and property of heat affected zone of crack-free steel Q500CF weld joint GUO Huiying, ZHANG Yu, HE Yuchun, XU Hongmei (Institute of Research of Iron and Steel, Shasteel, Zhangjiagang 215625, China). pp 108-112

Abstract: The effect of heat input on microstructure and impact property of heat affected zone (HAZ) of crack-free steel plate Q500CF was examined by using submerged arc welding (SAW) test and Gleeble simulation. It is found that, SAW joint show excellent impact property in HAZ ($A_{KV,-20\,℃} \geqslant 146$ J) with heat input between 15 and 50 kJ/cm. Among HAZ, fusion boundary (FL) have the lowest impact value, which decreases with heat input increases. Coarse grained HAZ microstructure of SAW joint changed from a mixture of lath bainite (LB) and granular bainite (GB) at heat input of 15 kJ/cm to a single GB structure at heat input of 50 kJ/cm. A large amount of 1 ~ 7 μm M-A constituents are formed at prior austenite grain boundary at inter-critical coarse grained HAZ, resulting in impact toughness deterioration of this region. Gleeble simulation results show that higher heat input of 50 ~ 70 kJ/cm causes coarsening of GB, which decreases impact toughness of coarse grained HAZ. In conclusion, heat input should be restricted to 15 ~ 50 kJ/cm for sake of impact property of HAZ.

Key words: crack-free steel plate; submerged arc welding; coarse grained heat affected zone; Gleeble simulation; impact property